

# Moving solvated electrons with light: Nonadiabatic mixed quantum/classical molecular dynamics simulations of the relocalization of photoexcited solvated electrons in tetrahydrofuran (THF)

Michael J. Bedard-Hearn, Ross E. Larsen,<sup>a)</sup> and Benjamin J. Schwartz<sup>b)</sup>

*Department of Chemistry and Biochemistry, University of California, Los Angeles,  
Los Angeles, California 90095-1569*

(Received 11 July 2006; accepted 5 September 2006; published online 16 November 2006)

Motivated by recent ultrafast spectroscopic experiments [Martini *et al.*, *Science* **293**, 462 (2001)], which suggest that photoexcited solvated electrons in tetrahydrofuran (THF) can relocalize (that is, return to equilibrium in solvent cavities far from where they started), we performed a series of nonequilibrium, nonadiabatic, mixed quantum/classical molecular dynamics simulations that mimic one-photon excitation of the THF-solvated electron. We find that as photoexcited THF-solvated electrons relax to their ground states either by continuous mixing from the excited state or via nonadiabatic transitions,  $\sim 30\%$  of them relocalize into cavities that can be over 1 nm away from where they originated, in close agreement with the experiments. A detailed investigation shows that the ability of excited THF-solvated electrons to undergo photoinduced relocalization stems from the existence of preexisting cavity traps that are an intrinsic part of the structure of liquid THF. This explains why solvated electrons can undergo photoinduced relocalization in solvents like THF but not in solvents like water, which lack the preexisting traps necessary to stabilize the excited electron in other places in the fluid. We also find that even when they do not ultimately relocalize, photoexcited solvated electrons in THF temporarily visit other sites in the fluid, explaining why the photoexcitation of THF-solvated electrons is so efficient at promoting recombination with nearby scavengers. Overall, our study shows that the defining characteristic of a liquid that permits the photoassisted relocalization of solvated electrons is the existence of nascent cavities that are attractive to an excess electron; we propose that other such liquids can be found from classical computer simulations or neutron diffraction experiments. © 2006 American Institute of Physics. [DOI: 10.1063/1.2358131]

## I. INTRODUCTION

Solvated electrons have long held a special interest in condensed-phase physical chemistry because their behavior provides intimate contact between ultrafast spectroscopic experiments<sup>1-5</sup> and quantum molecular dynamics simulations.<sup>6-16</sup> Although simulations have been able to explain the spectrum of equilibrated solvated electrons in a variety of solvents,<sup>6,15,17-20</sup> including tetrahydrofuran (THF),<sup>21</sup> there still remain open questions concerning the behavior and dynamics of photoexcited solvated electrons. For example, in recent work Martini *et al.* created THF-solvated electrons ( $e_{\text{THF}}^-$ ) via photodetachment from  $\text{Na}^-$ .<sup>22,23</sup> Upon excitation of the  $e_{\text{THF}}^-$ , Martini *et al.* found that the amount of geminate recombination of electrons with their parent Na atoms was altered compared to electrons that had not been excited. Moreover, these workers found that depending on when the excitation pulse was applied after the photodetachment process, geminate recombination could be either enhanced or diminished, suggesting that when photoexcited THF-solvated electrons return to their ground state, a significant fraction of them occupy a new physical location in the liquid. In other words, the excitation pulse caused

THF-solvated electrons to *relocalize* and transfer to a new location at least one solvent shell away.<sup>22,23</sup>

In contrast, the behavior and dynamics of photoexcited *hydrated* electrons are very different compared to the  $e_{\text{THF}}^-$ . Son *et al.* photoexcited solvated electrons in water and found that recombination could be enhanced by excitation into the blue edge of the hydrated electron's absorption spectrum, but not by excitation near the maximum or on the red side of the absorption band.<sup>24</sup> These authors suggested that photoexcitation of hydrated electrons can promote reactions with nearby scavengers while the electron is in a continuum state (i.e., while the electron's wave function is delocalized), but their experiments found no evidence that the subsequent relaxation of excited hydrated electrons led to relocalization. This experimental result contradicts an earlier idea put forward by Funabashi *et al.* who, based on a semicontinuum model, suggested that the photoexcitation of hydrated electrons could lead to relocalization into new trapping sites.<sup>25</sup> In this paper, we propose an explanation for why photoexcitation causes solvated electrons to move in solvents like THF but not in solvents like water.

In a previous work, we examined the nature of the THF-solvated electron by performing equilibrium, adiabatic (Born-Oppenheimer) mixed quantum/classical (MQC) molecular dynamics (MD) simulations.<sup>21</sup> We found that (like

<sup>a)</sup>Electronic mail: rlarsen@chem.ucla.edu

<sup>b)</sup>Electronic mail: schwartz@chem.ucla.edu

hydrated electrons<sup>6,8,14</sup>), the ground state of the  $e_{\text{THF}}^-$  is a quasispherical species bound in a “primary” solvent cavity, here defined as the cavity that contains the adiabatic ground-state wave function, regardless of whether or not the solvated electron is in its ground state. Also similar to what is observed for hydrated electrons, the first two excited states of the  $e_{\text{THF}}^-$  are localized in the primary cavity and have  $p$ -like symmetry. Unlike the hydrated electron, however, we found that higher-lying excited states of the THF-solvated electron can occupy one or more of the numerous “secondary” cavities in the liquid, which we define as any cavity in the solvent that does not contain the adiabatic ground state. We determined that the existence of secondary cavities is an intrinsic property of the way the THF molecules pack in the condensed phase, and that even in the neat solvent these naturally occurring cavities are positively polarized and thus act as traps for an excess electron.<sup>21</sup> Our prediction of the existence of these partially polarized cavities in neat THF was recently verified in neutron diffraction experiments by Bowron *et al.*<sup>26</sup> We also found that because of fluctuations, sometimes electronic states in the secondary cavities can be lower in energy than the higher-lying  $p$ -like states in the primary cavity.<sup>21</sup>

In this paper, we use nonadiabatic (non-Born-Oppenheimer) MQC MD simulations to show that the presence of secondary cavities in liquid THF is directly responsible for the relocation of THF-solvated electrons following photoexcitation. We find that an excited solvated electron in THF, even one excited entirely within the primary cavity, has a significant probability to relax into one of the secondary cavities, which can be over 1 nm away from the primary cavity that the electron started in; this mechanism is similar in spirit to that proposed in Ref. 25. Our results also explain why photoinduced electron relocation occurs in THF but not in water: Water lacks the preexisting electron traps found in THF that act to stabilize the excited-state solvated electron in a new cavity following excitation. The rest of this paper is organized as follows: The next section discusses our computational methods and analytical techniques, the third section presents the results of our simulations, and the last section provides a comparison of our results to experiment as well as a general discussion and conclusions.

## II. COMPUTATIONAL METHODS

The nonadiabatic mixed quantum/classical molecular dynamics simulations discussed here used 255 classical THF solvent molecules and a single quantum mechanical excess electron interacting in a cubic box of side 32.5 Å with periodic boundary conditions. The excess electron interacts with periodic images of all of the THF molecules, but does not interact with images of itself, so there is no spurious electron-electron interaction in this charged system. The simulations were performed in the microcanonical ensemble, and the classical equations of motion were integrated using the Verlet algorithm.<sup>27</sup> The rigid, five-site classical THF solvent molecules interacted through a potential developed by Jorgensen that consists of Lennard-Jones and Coulomb interactions,<sup>28–30</sup> with the potential tapered smoothly to zero

at half the box length.<sup>31</sup> For the quantum mechanical electron, we solved the time-independent Schrödinger equation using the Hamiltonian  $\hat{H}=\hat{T}+\hat{V}_p$ , where  $\hat{T}$  is the kinetic energy operator and  $\hat{V}_p$  is a pairwise additive THF-electron pseudopotential, which, depends on the separation between the electron and each of ten interaction centers (the five united-atom sites plus the five bond midpoints) on every THF molecule; we have described this pseudopotential in detail previously.<sup>21</sup> At each time step of the simulation, we solved the Schrödinger equation for the six lowest adiabatic eigenstates  $|\phi_k\rangle$  and eigenvalues  $\varepsilon_k$  on an evenly spaced  $24 \times 24 \times 24$  cubic grid using an iterative and block Lanczos algorithm,<sup>32</sup> assuring that for each state,  $\langle \phi_k | \hat{H} | \phi_k \rangle - \varepsilon_k \leq 10 \mu\text{eV}$ . Upon excitation, we calculated the nonadiabatic relaxation dynamics of the THF-solvated electron using the mean field with stochastic decoherence (MF-SD) algorithm.<sup>33</sup> In MF-SD, the quantum subsystem is described by a mean-field (MF) wave function that is a superposition of the adiabatic eigenstates,

$$|\psi_{\text{MF}}\rangle = \sum_{k=0}^5 a_k |\phi_k\rangle, \quad (1)$$

whose expansion coefficients  $a_k$  evolve in time according to the time-dependent Schrödinger equation. We chose the nonadiabatic coupling width parameter<sup>33,34</sup> for MF-SD to be  $w=4$  Å; a justification for this choice, along with other details of how the simulations were carried out, will be presented in a forthcoming paper.<sup>35</sup>

To investigate the possible relocation of photoexcited THF-solvated electrons, we performed 32 nonequilibrium, nonadiabatic trajectories, each of which simulated a one-photon Franck-Condon excitation of the  $e_{\text{THF}}^-$ . To mimic what is done in femtosecond pump-probe experiments, an equilibrated THF-solvated electron was promoted at time  $t=0$  from the ground state into one of the adiabatic excited states  $k$  chosen such that the energy gap between the ground and excited state was  $\varepsilon_{k0}=\varepsilon_k-\varepsilon_0=1.45\pm 0.05$  eV, which is near the peak of the THF-solvated electron’s calculated absorption spectrum for our model.<sup>21</sup> The starting configurations for the simulations presented here were taken from three distinct sections of a 40 ps equilibrium trajectory,<sup>21</sup> with each of the three sections separated by  $\sim 10$  ps; nineteen of our starting configurations came from a 6 ps section of our equilibrium trajectory, nine came from a 5 ps section, and four came from a 1 ps section.<sup>36</sup> The average separation between any two sequential configurations within each of the three sections was  $\sim 320$  fs and no two initial configurations were separated by less than 200 fs.

Following excitation, the electron eventually reached the adiabatic ground state in one of two ways: Either the coherent superposition state  $|\psi_{\text{MF}}\rangle$  that describes the quantum subsystem experienced a decoherence event and instantaneously collapsed to the adiabatic ground state as prescribed by the MF-SD algorithm,<sup>33,37</sup> which we refer to as “nonadiabatic relaxation,” or the mixed state continuously transferred population to the ground state; we refer to this latter mechanism as “diabatic relaxation.” Although the term “diabatic” is usually used to refer to stationary states or states that are

fixed in space, here we use the term to describe the nearly stationary mean-field excited state that resides in a nearly stationary solvent cavity. Hence, we use the phrase diabatic relaxation when we refer to the continuous transfer of population between the various adiabatic states, which allows the mean-field wave function  $|\psi_{MF}\rangle$  to remain in a single cavity as it relaxes to the ground state; in other words, the mean-field wave function has the character of a diabatic state chosen to occupy a single cavity. Finally, to ensure that the MQC system had fully reequilibrated following either diabatic or nonadiabatic relaxation, we ran all of our simulations for at least 3 ps after the electron reached the ground state.<sup>38</sup>

The distinguishing characteristic of photoinduced relocalization is whether or not the solvated electron, after it reequilibrates on the ground state, occupies the same solvent cavity as the one from which it started. If the relaxed electron does not occupy the same cavity from which it was photoexcited, then it must have moved into a new solvent cavity. We determined whether or not the excited electron relaxed into a new solvent cavity by calculating the overlap of the electron's adiabatic ground-state wave function at the instant of excitation,  $t=0$ , with the adiabatic ground-state wave function at some later time  $t$ :

$$\zeta(t) = \langle \phi_0(t) | \phi_0(0) \rangle. \quad (2)$$

If relocalization does occur, then we expect the overlap  $\zeta$  to decay nearly to zero. On the other hand, if the electron reaches the ground state in the same solvent cavity from which it originated (that is, if the  $e_{\text{THF}}^-$  does not relocalize), then the overlap should be near unity after the electron reaches the ground state.

### III. RESULTS: NONADIABATIC MQC SIMULATIONS OF PHOTOEXCITED THF-SOLVATED ELECTRONS

In our previous studies of the  $e_{\text{THF}}^-$ , we found that there were three qualitatively different types of states to which the  $e_{\text{THF}}^-$  could be excited; Fig. 1 shows examples (chosen from three different equilibrium solvent configurations) of the different kinds of excited states, and Table I gives the frequency with which each type of excitation occurred in our nonequilibrium ensemble. In Fig. 1, the blue wire mesh surfaces show isodensity contours of the adiabatic ground state and the red solid surfaces are isodensity contours for selected adiabatic excited states whose energy is  $1.45 \pm 0.05$  eV above the ground state.<sup>39</sup> The first kind of excitation available at this energy promotes the  $e_{\text{THF}}^-$  from an  $s$ -like ground state to a  $p$ -like excited state and takes place entirely within the primary cavity, as illustrated in Fig. 1(A). Table I shows that creation of an initial  $p$ -like excited state in the primary cavity is the most common type of excitation in our ensemble. Since these transitions occur between states with a large amount of spatial overlap, their absorption cross sections are relatively large and thus they constitute the majority of the THF-solvated electron's absorption spectrum.<sup>21</sup> The second type of excitation available to the  $e_{\text{THF}}^-$  at this energy has two states that have charge density in multiple cavities simultaneously, including the primary cavity, as shown in Fig. 1(B). The oscillator strength for transitions to such multiple-cavity

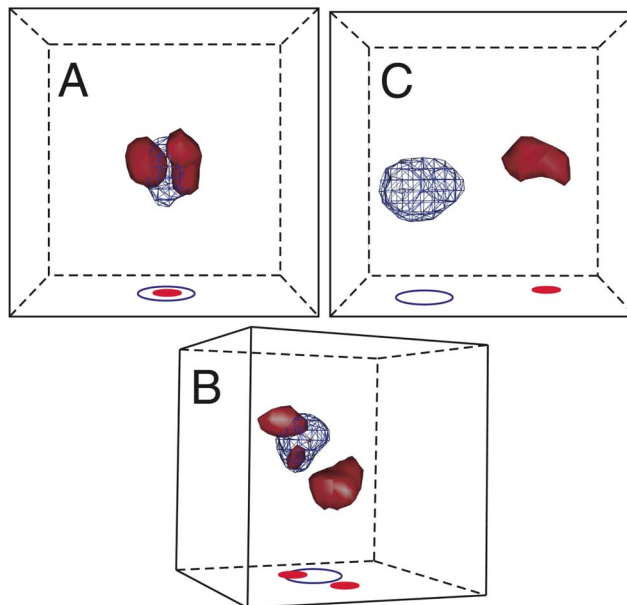


FIG. 1. Charge densities from three different equilibrium solvent configurations illustrating the three different types of excitation (solid red surfaces) available to the THF-solvated electron (Ref. 39). The electron always begins in an  $s$ -like ground state in the primary cavity (blue wire meshes) and can be excited either to a  $p$ -like state within the primary cavity (A), a multiple-cavity state (B), or a totally disjoint state (C), see text and Table I for details. The bounding box indicates the 32.5 Å size of the simulation cell. The drop shadows [open blue circle for the ground state and solid red circle(s) for the excited state], placed underneath the center of mass of each state's major lobes, are meant to aid in depth perception and do not convey size information.

states, however, is lower by a factor of  $\sim 4$  relative to the  $s$ -to- $p$ -like transitions (see Table I). Finally, at this energy the THF-solvated electron can occasionally make a transition from the ground state to a disjoint excited state, whose charge density is almost entirely in one or more of the secondary cavities, as shown in Fig. 1(C), such states have a minimal amount of overlap with the ground state, and thus their transition dipoles are quite weak. Experimentally, transitions of this type are unlikely to take place, and in our simulations, they represent only a small fraction of our nonequilibrium ensemble. Table I displays the average transition dipole moment  $M_{0k}$  to each type of initial excited state,

$$M_{k0} = \varepsilon_{k0} \langle \phi_k | \hat{\mathbf{r}} | \phi_0 \rangle, \quad (3)$$

and summarizes the number of trajectories from each type of excitation that underwent relocalization. As discussed below,

TABLE I. Number of trajectories in the nonequilibrium ensemble starting in each of the different types of excited state (cf. Fig. 1) and the fraction from each type that ends in electron relocalization.

Excitation type	Number (% of ensemble)	$\langle M_{k0} \rangle$ eV Å <sup>2</sup>	Number relocalized (% of type)
$s \rightarrow p$	18 (56)	2.85 <sup>a</sup>	4 (22)
$s \rightarrow$ multiple cavity	11 (34)	0.68 <sup>a</sup>	3 (27)
$s \rightarrow$ disjoint	3 (9)	0.07 <sup>a</sup>	2 (67)

<sup>a</sup>Ensemble-averaged time-zero transition dipole moments  $\langle M_{k0} \rangle$  were calculated via Eq. (3).

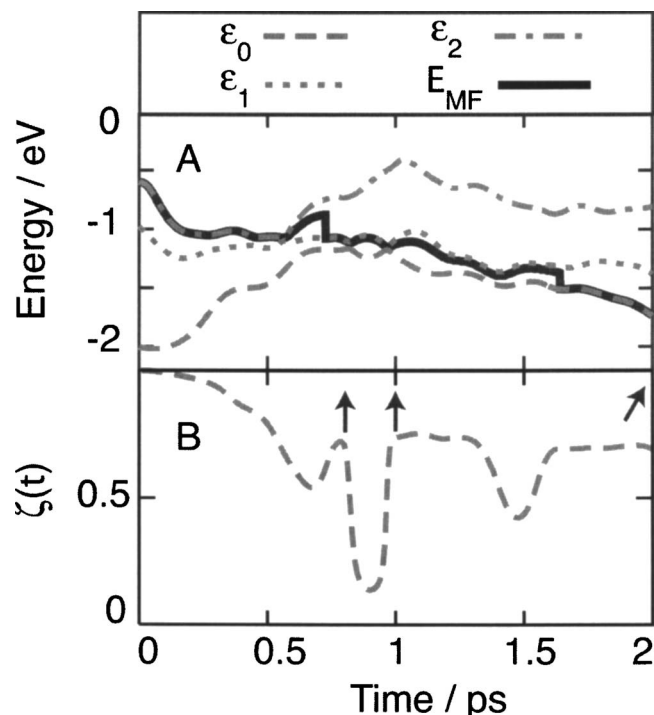


FIG. 2. Representative nonequilibrium trajectory in which the excited THF-solvated electron is promoted to a  $p$ -like excited state in the primary cavity and does not undergo relocalization. (A) shows the time evolution of the three lowest adiabatic eigenenergies (gray dashed and dotted curves) and the mean-field energy,  $E_{MF}$  (solid black curve). (B) shows the time evolution of the adiabatic ground-state overlap integral, Eq. (2). The arrows indicate the times for which the charge densities of the adiabatic ground and mean-field states are shown in Figs. 3(A)–3(C) below.

we defined trajectories as having relocalized if  $\zeta(t) < 0.05$  for all times after the photoexcited electron has reached the adiabatic ground state.<sup>38</sup>

Figure 2 shows a representative trajectory from the non-equilibrium ensemble in which the  $e_{THF}^-$  is promoted to its second excited state, in this case a  $p$ -like state in the primary cavity similar to that shown in Fig. 1(A). Figure 2(A) shows the dynamical history of the three lowest adiabatic eigenvalues  $\varepsilon_k$  (various gray dotted and dashed curves) and the mean-field energy,  $E_{MF} = \langle \psi_{MF} | \hat{H} | \psi_{MF} \rangle$  (thick black solid curve). Although the electron is initially promoted into its second excited state, after  $\sim 500$  fs the solvent induces mixing with the first excited state, and then at  $t \approx 750$  fs, the mean-field wave function decoheres (undergoes a nonadiabatic collapse) to the first excited state. Once on the first excited state, solvent motions cause additional mixing, now with the adiabatic ground state, and the system makes a nonadiabatic transition to the ground state at  $t = 1.65$  ps. The majority of our non-equilibrium trajectories followed this same general pattern. After excitation, the electronic wave function mixed with progressively lower-lying excited states, came to a quasi-equilibrium on the first excited state (which is generally a  $p$ -like excited state in the original primary cavity), and finally collapsed nonadiabatically to the ground state in the primary cavity.

Figure 2(B) displays the ground-state overlap integral,  $\zeta(t)$  [Eq. (2)], which shows clearly that the reequilibrated ground-state wave function looks much the same as it did

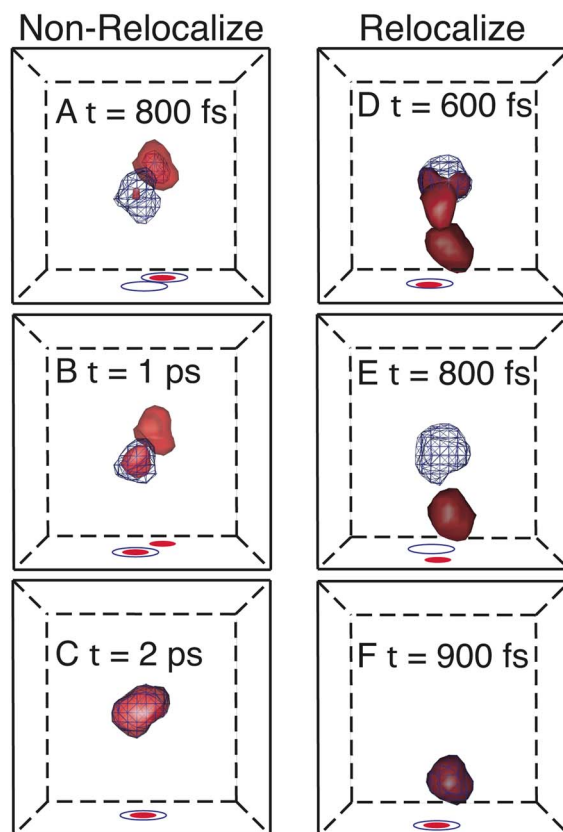


FIG. 3. Adiabatic ground (blue mesh surfaces) and mean-field state (solid red surfaces) charge densities for selected configurations from two representative nonequilibrium excited-state trajectories of the THF-solvated electron, with the same conventions as in Fig. 1. The charge densities (Ref. 39) shown in (A)–(C) are for configurations at a few select times for the trajectory shown in Fig. 2, and the charge densities shown in (D)–(F) are for trajectory shown in Fig. 4. Although it is obscured by the red surface representing the mean-field charge density, the adiabatic ground state in panel (A) occupies two cavities, as indicated by the two blue-ring drop shadows.

prior to excitation. At early times, the overlap is near unity and shows only a slow, small decay over the first  $\sim 0.5$  ps, which we attribute to simple diffusive motion of the primary cavity from its  $t=0$  location.<sup>40</sup> After  $\sim 1.7$  ps, when the electron has reached the ground state, the overlap remains high ( $\zeta \approx 0.7$ ), verifying that the newly relaxed electron occupies the same solvent cavity as the one from which it was originally excited. Despite this clear indication that the electron in this trajectory did not relocalize, Fig. 2(B) shows that at  $t \approx 800$  fs, the overlap  $\zeta(t)$  briefly decayed to a low value of  $\sim 0.1$  before recovering at  $t \approx 1$  ps. This suggests that the ground-state wave function had temporarily moved into a new cavity, but returned to the primary cavity by  $t \approx 1$  ps.

To better understand this event, panels (A), (B), and (C) of Fig. 3 display charge densities of the mean-field state (red solid surfaces) and the adiabatic ground state (blue wire meshes) for a few select configurations in this trajectory indicated by the arrows in Fig. 2.<sup>39</sup> Figure 3(A) verifies that although the electron was initially excited within the primary cavity, the mean-field wave function at  $t=800$  fs is almost entirely localized in a secondary cavity. Moreover, the electron's adiabatic ground state now occupies two solvent cavities that are in different places in the fluid. The adiabatic

ground state simultaneously occupies *both* the original primary cavity and the secondary cavity that is occupied by the excited electron. Evidently, solvent motions working to relax the mean-field excited state have made the two cavities quasidegenerate, causing the adiabatic ground state to be shared by both cavities. Although the mean-field state now occupies a new cavity, the solvent motions that lowered the energy of the secondary cavity relative to the primary cavity do not persist. By  $t=1$  ps [Fig. 3(B)], the primary cavity is again more attractive to the electron; this causes the adiabatic ground state to move back entirely within the original primary cavity [as suggested by the recovery of  $\zeta(t)$  seen in Fig. 2(B)] and the mean-field charge density to start moving back to the primary cavity from the secondary cavity. After the nonadiabatic transition to the ground state occurs at  $t = 1.65$  ps, the mean-field wave function becomes essentially identical to the ground-state wave function, and both occupy the original cavity [panel (C)]; thus, for this trajectory, no relocalization is observed. We find that in almost every one of our nonequilibrium trajectories, even those that do not ultimately lead to relocalization, the excited electron tends to leak out of the primary cavity temporarily but eventually returns to the first excited state in the primary cavity, where it remains for roughly 1–3 ps before collapsing to the original ground state. Thus, even though the majority of our trajectories do not show relocalization, the photoexcited  $e_{\text{THF}}^-$  does have the opportunity to visit other cavities in the liquid before relaxing to the ground state.

Can the fact that excited THF-solvated electrons spend time in secondary cavities sometimes lead to relocalization? In Figs. 3(D)–3(F) and 4 we show a representative trajectory in which the photoexcited THF-solvated electron's relaxation follows a different path than that in Fig. 2. The electron is initially placed in its fourth excited state, in this case the high-lying *p*-like state in the primary cavity that is shown in Fig. 1(A), but in this trajectory the excited electron undergoes diabatic relaxation to return to the ground state. The trajectory shown in Fig. 4 begins much the same as the trajectory shown in Fig. 2, with solvent motions inducing the excited state to mix with the lower-lying adiabatic excited states. After  $\sim 600$  fs, these solvent motions have caused the mean-field state to develop a large lobe of charge that extends into a secondary cavity whose center is nearly 12 Å away from that of the primary cavity, as shown explicitly in Fig. 3(D). At  $t \approx 750$  fs, the electron collapses to the first adiabatic excited state, and after a few more femtoseconds the mean-field wave function becomes localized entirely in the secondary cavity, as shown in Fig. 3(E).<sup>41</sup> Up to this point, the two trajectories in Figs. 2 and 4 have behaved quite similarly. From here, however, the two trajectories qualitatively diverge: For the trajectory shown in Fig. 4, the ensuing solvent motions around the charge in the secondary cavity respond to better accommodate the  $e_{\text{THF}}^-$ , while those around the primary cavity continue to become less favorable. This solvation continues until the secondary cavity becomes lower in energy than the primary cavity, leading to a diabatic crossing at  $t \approx 900$  fs; after this crossing, the electron is now in the ground state in a new primary cavity that is almost 12 Å away from where it started [Fig. 3(F)].

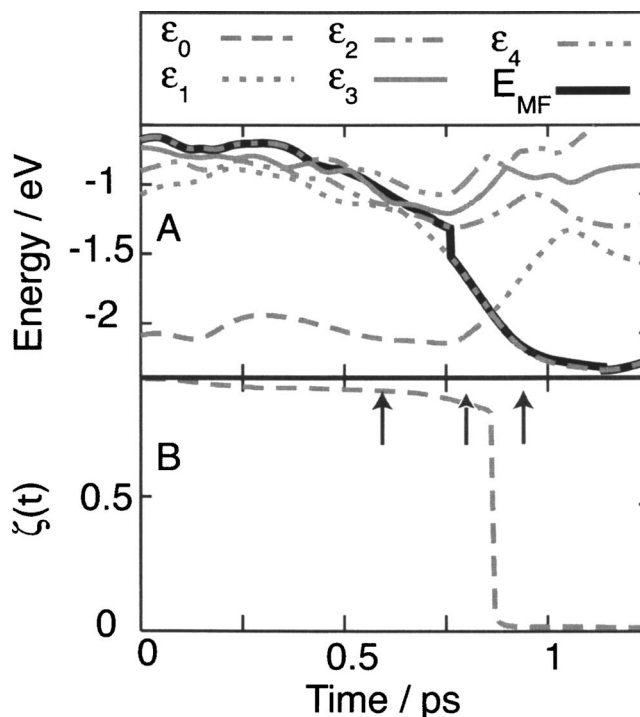


FIG. 4. Representative nonequilibrium trajectory in which the excited THF-solvated electron is promoted to the *p*-like excited state shown in Fig. 1(A) in the primary cavity and eventually undergoes relocalization. (A) shows the time evolution of the five lowest adiabatic eigenvalues (gray dashed and dotted curves) and the mean-field energy  $E_{\text{MF}}$ ; the curve crossing visible at  $t \approx 900$  fs does not involve a nonadiabatic transition (see text for further details). (B) shows the time evolution of the adiabatic ground-state overlap integral, Eq. (2), which decays instantaneously to near zero at the moment the electron diabatically reaches the ground state. The arrows indicate the times for which the charge densities of the adiabatic ground and mean-field states are shown in Figs. 3(D)–3(F).

The fact that this trajectory provides an example of photoinduced relocalization of the THF-solvated electron is verified in Fig. 4(B), which shows the time-dependent overlap of the adiabatic ground state  $\zeta(t)$  [Eq. (2)]. At the point of the diabatic crossing at  $t \approx 900$  fs,  $\zeta(t)$  decays almost instantaneously from near unity to  $\sim 0.02$ . This happens because the ground-state wave function moves to a different location than the one it started in, and unlike what was seen in Fig. 2, the ground state never returns to the primary cavity. Thus, Fig. 4 offers a definitive example of photoinduced relocalization, where excitation of the  $e_{\text{THF}}^-$  within the primary cavity (which occurs with high oscillator strength and thus with high probability) caused the THF-solvated electron to move  $\sim 12$  Å from where it started in under 1 ps, a time orders of magnitude faster than what could be expected from diffusion.

The near step-function decay of  $\zeta$  to  $< 0.05$  without subsequent recovery seen in Fig. 4(B) is common to all nine of our nonequilibrium trajectories that underwent relocalization. It is worth noting that in a few of our nonequilibrium trajectories in which the photoexcited electron did not relocalize, the ground-state wave function did undergo temporary relocalization *before* reequilibration. These events look much like the partial relocalization seen in Fig. 2,  $t \approx 800$  fs, except that instead of being shared by two cavities as in Fig. 2(D), the ground state became fully localized in a

new cavity. This caused  $\zeta(t)$  to decay to near zero with the same step-function-like behavior seen in Fig. 4(B). In these few cases, however, the relocalization of the ground state was only temporary and by the time the excited  $e_{\text{THF}}^-$  reached the ground state, it had returned to the original primary cavity, thus leading to a recovery of  $\zeta(t)$ . Table I shows that relocalization can occur following excitation into any of the three different types of excited states depicted in Fig. 1. The table also suggests that the probability of undergoing relocalization increases with the extent to which the initially occupied excited state is delocalized into one or more of the secondary cavities, although the statistics are too poor for a definitive conclusion. Moreover, the average transition dipole moment at  $t=0$  for the nine trajectories in which we observed relocalization was  $1.5 \text{ eV \AA}^2$  [see Eq. (3) and Table I], which suggests that the kinds of photoexcitations that eventually lead to relocalization of THF-solvated electrons are indeed experimentally accessible.

In addition to the three excitations to disjoint cavities from our nonequilibrium ensemble, we ran two additional trajectories at higher excitation energy in order to better sample the dynamics of the  $e_{\text{THF}}^-$  excited directly into states that occupy disjoint cavities, such as that in Fig. 1(C). In both of these additional trajectories, the transition dipole moments were extremely small (as in Table I) though nonzero, and both of the higher excitations led to relocalization. Thus, although our nonequilibrium ensemble is small, our results certainly suggest that relocalization is enhanced when the electron is excited into multiple-cavity or disjoint excited states.

As seen in the two example trajectories shown in Figs. 2 and 4, the mean-field wave function of the excited  $e_{\text{THF}}^-$  can reach the ground state via either nonadiabatic wave function collapse (decoherence) or through continuous (diabatic) population transfer; we found that decoherence was the preferred relaxation mechanism in the 23 trajectories in which the excited  $e_{\text{THF}}^-$  did not relocalize. For these 23 trajectories, the excited  $e_{\text{THF}}^-$  behaves largely in the same manner as the excited hydrated electron, which also reaches a quasiequilibrium on the first excited state and remains there until a solvent fluctuation induces the excited-state wave function to collapse onto the ground state;<sup>34</sup> the one significant difference is that the excited hydrated electron never leaves its primary cavity,<sup>14</sup> whereas we see significant leakage of the THF-solvated electron's wave function into secondary cavities during relaxation.

#### IV. DISCUSSION: RELOCALIZATION OF PHOTOEXCITED THF-SOLVATED ELECTRONS

The fact that the excited-state wave function of the  $e_{\text{THF}}^-$  leaks into secondary cavities but the hydrated electron's wave function does not is what allows a significant fraction of excited solvated electrons to relocalize in THF but not in water. The origin of this difference in the behavior and dynamics between hydrated electrons and THF-solvated electrons is that the excited  $e_{\text{THF}}^-$  can sample secondary cavities because THF solvent molecules pack poorly in the liquid, which creates many voids that are prearranged to help stabi-

lize the solvated electron and facilitate relocalization. The structure of liquid water, however, presents no such preexisting attractive cavities<sup>42</sup> and thus offers no opportunities for excited hydrated electrons to relocalize. The leakage of the THF-solvated electron's wave function into secondary cavities also means that unlike the hydrated electron, the excited  $e_{\text{THF}}^-$  need not remain in the first excited state waiting for decoherence to induce a collapse back to the ground state. Rather, continuous solvation of the  $e_{\text{THF}}^-$  in a secondary cavity can bring the system back to the ground state without a nonadiabatic transition, as seen in Fig. 4.

In our study, the fraction of trajectories in which we see the excited  $e_{\text{THF}}^-$  undergo relocalization is remarkably consistent with the femtosecond pump-probe experiments that originally suggested electron relocalization in THF.<sup>22,23</sup> In the experiments, THF-solvated electrons located one solvent shell away from a solvated Na atom were photoexcited near the electron's absorption maximum. Roughly one-half of the excited electrons underwent rapid recombination with their parent Na atoms during the time that the electron was in its excited state (as measured by the recovery of the THF-solvated electron's ground-state bleach). This suggests that the excited electrons were easily able to sample the cavity containing the parent Na atom a few angstroms away, consistent with our findings that the excited  $e_{\text{THF}}^-$  sampled secondary cavities in virtually *all* of our trajectories, even those that did not ultimately show relocalization [cf. Figs. 2, 3(A), and 3(B)]. From their experiments, Martini, *et al.* found that roughly one-third of the remaining photoexcited electrons (the ones that did not directly recombine with their Na atom partners) appeared to relocalize, as judged by the change in recombination dynamics for this fraction of the population.<sup>22,23</sup> If we ignore the experimental fraction of excited solvated electrons that underwent direct photoinduced recombination (because there are no Na atoms in our simulations), then the experimentally observed ratio of one-third of the remaining electrons that underwent photoinduced relocalization is in excellent agreement with the  $\sim 30\%$  that we see in our simulations (cf. Table I).

Although the simulated fraction of excited electrons that undergo relaxation is in excellent agreement with experiment, the simulated excited-state lifetimes agree less well with experiment. We find that for the nine trajectories in which electrons relocalized, the electron took  $\sim 2.5 \pm 0.7$  ps to relax to the ground state, and that the entire 32-member ensemble of trajectories had an average lifetime of  $\sim 3.7 \pm 0.5$  ps. These lifetimes are far slower than the  $\sim 450$  fs relaxation time measured in femtosecond pump-probe experiments by Martini and Schwartz.<sup>43</sup> This difference in time scales, however, is not entirely unexpected for three reasons. First, nonadiabatic MQC simulations of other solvated electrons, such as the hydrated electron, are known to predict lifetimes longer than seen in experiment.<sup>34,44</sup> Second, the model THF-electron pseudopotential that we have employed, although qualitatively correct, is not rigorous;<sup>45</sup> if the potential we chose is too hard or too soft, this may affect the lifetime. Third, our rigid model of THF does not contain any high frequency intramolecular vibrational motions that are known to induce faster nonadiabatic transitions.<sup>46</sup>

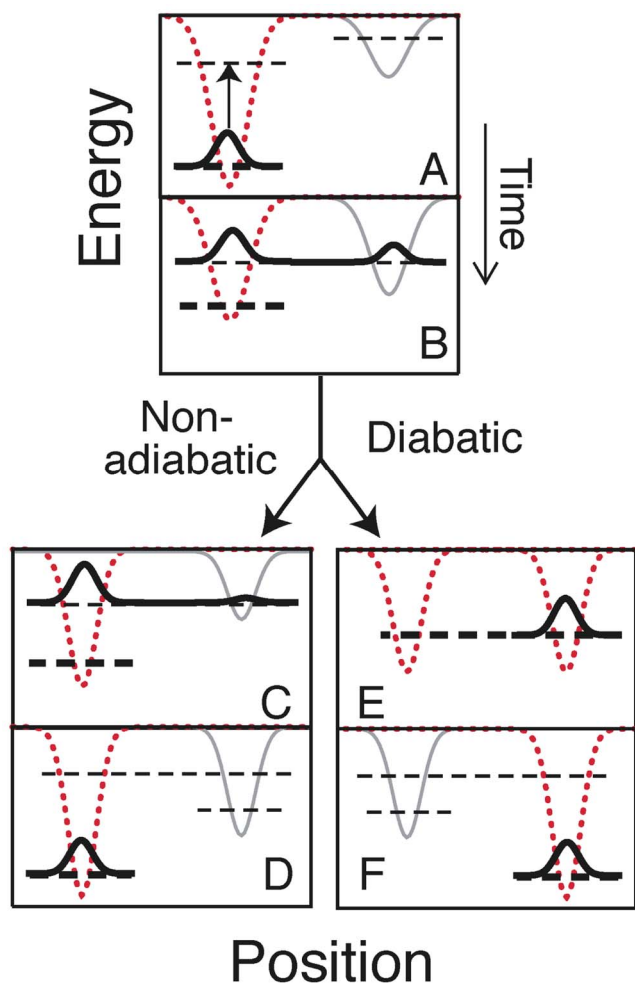


FIG. 5. Schematic illustration depicting the nonequilibrium relaxation of photoexcited solvated electrons in THF. In all six panels, the potential energy well of the primary cavity is depicted by a dotted red curve and that of a secondary cavity is shown as a solid gray curve; the mean-field electronic wave function is schematically illustrated by the thick solid curves (for simplicity, no nodes are shown); and the adiabatic ground- and excited-state energies are shown as the thick and thin dashed lines, respectively. See text for a detailed discussion of the two relaxation pathways shown.

To further illustrate how the presence of secondary cavities aids in electron relocalization, we present a schematic of the THF-solvated electron's excited-state relaxation dynamics in Fig. 5. Each panel depicts two solvent cavity traps, drawn as potential energy wells, for the excess electron; the red dotted curves represent the primary cavity and the gray solid curves represent a secondary cavity. The ground-state energy in each panel is indicated by the thick dashed lines, a few selected excited adiabatic energy levels are depicted by thin dashed lines, and the mean-field wave function is schematically represented by the solid black curves. Each panel illustrates the relaxation dynamics of the excited  $e_{\text{THF}}^-$  at a different time following the initial excitation, with time increasing from top to bottom. Panel (A) of Fig. 5 shows the initial adiabatic ground state (and the primary cavity) as starting on the left-hand side, and the vertical arrow indicates that the  $e_{\text{THF}}^-$  is typically excited within the primary cavity, as was the case in the examples shown in Figs. 2–4. As time progresses, part of the mean-field wave function leaks into a

secondary cavity [panel (B)], as discussed above; we note that this kind of multiple-cavity state may be reached either through dynamic solvation, as in Fig. 3(D) or via direct excitation to a state such as that shown in Fig. 1(B).

The system's subsequent evolution depends on precisely how the solvent responds to the presence (or absence) of charge in each of the two cavities. If the dominant effect of the solvent response is to restabilize the primary cavity, the electron will be “pulled” back into its initial cavity, or toward the left as illustrated in panel (C) of Fig. 5; this is exactly the type of behavior seen in the trajectory shown in Figs. 2 and 3(A)–3(C). When the mean-field wave function is pulled back into the primary cavity, the system typically reequilibrates via nonadiabatic collapse (decoherence) of the excited mean-field wave function onto the adiabatic ground state, so that no net relocalization occurs, as shown in panel (D). On the other hand, if solvent motions continue to stabilize the charged lobe in the secondary cavity, the excited electron may be driven out of the primary cavity and into the secondary cavity, or toward the right as in panel (E) of Fig. 5. Figure 5(E) illustrates the moment when the two cavities become degenerate and the ground state occupies both cavities (hence both are dotted and colored red), as with the diabatic crossing event seen at  $t \approx 900$  fs in Fig. 4. At this instant, the adiabatic ground state occupies both cavities, but strong mixing of the mean-field state keeps the electron in the cavity on the right. After this crossing, the mean-field wave function and adiabatic ground state both occupy the right-hand cavity, which had been the secondary cavity; this is much like the diabatic relaxation observed in Figs. 4 and 3(D)–3(F). Since relocalization has occurred, the primary cavity has also changed location, as illustrated by the shift of the red dotted curve to the right in Fig. 5(F). We note that even though the excited electrons that relocalized typically reached the ground state via diabatic relaxation in the secondary cavity, we saw three trajectories where the  $e_{\text{THF}}^-$  was trapped in an excited state when the adiabatic ground state had moved to occupy a newly stabilized primary cavity. The  $e_{\text{THF}}^-$  in these three trajectories then relaxed via a nonadiabatic transition [e.g., from one of the states indicated by the thin dashed lines in Fig. 5(F)] to the ground state, leading to relocalization.

In summary, we have shown that the presence of preexisting secondary cavities in liquid THF can cause roughly 30% of photoexcited THF-solvated electrons to relocalize and reequilibrate in solvent cavities far from where they originated, a result that is consistent with recent femtosecond pump-probe experiments.<sup>22,23</sup> We see that relocalization can occur whether or not the initial excitation takes place fully within the primary cavity (as opposed to a multiple-cavity state or a state in a cavity completely disjoint from the ground state). We also find that even in trajectories for which the electron does not relocalize, the excited electron still has the opportunity to sample one or more secondary cavities in the fluid, consistent with the fact that a significant fraction of the electrons in the experiment underwent direct photoinduced recombination.<sup>22,23</sup> For those trajectories that do relocalize, we see that the excited  $e_{\text{THF}}^-$  usually relaxes diabatically (by continuous solvation and population transfer) but

occasionally relaxes nonadiabatically (by discontinuous wave function collapse to the ground state) into its new cavity. Based on the results of our simulations, we speculate that electron relocalization should happen in any liquid that contains preexisting cavities that act as traps for an excess electron, such as other ethers or hexamethylphosphoramide (HMPA).<sup>47</sup> Finally, since we believe that the defining characteristic of a liquid that enables electron relocalization is the mere existence of attractive cavities, it should be possible to find such solvents using either classical equilibrium simulations or neutron diffraction experiments.<sup>26</sup>

## ACKNOWLEDGMENTS

This work was supported by the National Science Foundation under Grant No. CHE-0603766. One of the authors (B.J.S.) is a Camille and Henry Dreyfus Teacher-Scholar. The images in Figs. 1 and 3 were created using the UCSF CHIMERA package from the Computer Graphics Laboratory, University of California, San Francisco (supported by Grant No. NIH P41 RR-01081).<sup>39</sup>

<sup>1</sup>X. L. Shi, F. H. Long, and K. B. Eisenthal, *J. Phys. Chem.* **99**, 6917 (1995).

<sup>2</sup>M. S. Pshenichnikov, A. Baltuska, and D. A. Wiersma, *Chem. Phys. Lett.* **389**, 171 (2004).

<sup>3</sup>C. Silva, P. K. Walhout, P. J. Reid, and P. F. Barbara, *J. Phys. Chem. A* **102**, 5701 (1998).

<sup>4</sup>D. Madsen, C. L. Thomsen, J. Thorgersen, and S. R. Keiding, *J. Chem. Phys.* **113**, 1126 (2000).

<sup>5</sup>J. Lindner, A. N. Unterreiner, and P. Vohringer, *ChemPhysChem* **7**, 363 (2006).

<sup>6</sup>P. J. Rossky and J. Schnitker, *J. Phys. Chem.* **92**, 4277 (1988).

<sup>7</sup>D. F. Coker, B. J. Berne, and D. J. Thirumalai, *Chem. Phys.* **86**, 5689 (1987).

<sup>8</sup>E. Neria, A. Nitzan, R. N. Barnett, and U. Landman, *Phys. Rev. Lett.* **67**, 1011 (1991).

<sup>9</sup>K. Leung and D. Chandler, *Annu. Rev. Phys. Chem.* **45**, 557 (1994).

<sup>10</sup>K. F. Wong and P. J. Rossky, *J. Phys. Chem. A* **105**, 2546 (2001).

<sup>11</sup>M. Boero, M. Parrinello, K. Terakura, T. Ikeshoji, and C. C. Liew, *Phys. Rev. Lett.* **90**, 226403 (2003).

<sup>12</sup>A. Staib and D. Borgis, *J. Chem. Phys.* **104**, 9026 (1996).

<sup>13</sup>C. Nicolas, A. Boutin, B. Levy, and D. Borgis, *J. Chem. Phys.* **118**, 9689 (2003).

<sup>14</sup>B. J. Schwartz and P. J. Rossky, *J. Chem. Phys.* **101**, 6902 (1994).

<sup>15</sup>B. J. Schwartz and P. J. Rossky, *J. Chem. Phys.* **101**, 6917 (1994).

<sup>16</sup>B. J. Schwartz and P. J. Rossky, *Phys. Rev. Lett.* **72**, 3282 (1994).

<sup>17</sup>L. Turi, A. Mosyak, and P. J. Rossky, *J. Chem. Phys.* **107**, 1970 (1997).

<sup>18</sup>J. Zhu and R. I. Cukier, *J. Chem. Phys.* **98**, 5679 (1993).

<sup>19</sup>M. Mitsui, N. Ando, S. Kokubo, A. Nakajima, and K. Kaya, *Phys. Rev. Lett.* **91**, 153002 (2003).

<sup>20</sup>E. Gallicchio and B. J. Berne, *J. Chem. Phys.* **105**, 7064 (1996).

<sup>21</sup>M. J. Bedard-Hearn, R. E. Larsen, and B. J. Schwartz, *J. Chem. Phys.* **122**, 134506 (2005).

<sup>22</sup>I. B. Martini, E. R. Barthel, and B. J. Schwartz, *Science* **293**, 462 (2001).

<sup>23</sup>I. B. Martini, E. R. Barthel, and B. J. Schwartz, *J. Am. Chem. Soc.* **124**, 7622 (2002).

<sup>24</sup>D. H. Son, P. Kambhampati, T. W. Kee, and P. F. Barbara, *J. Phys. Chem. A* **105**, 8629 (2001).

<sup>25</sup>K. Funabashi, I. Carmichael, and W. H. Hamill, *J. Chem. Phys.* **69**, 2652 (1978).

<sup>26</sup>D. T. Bowron, J. L. Finney, and A. K. Soper, *J. Am. Chem. Soc.* **128**, 5119 (2006).

<sup>27</sup>M. P. Allen and D. J. Tildesley, *Computer Simulation of Liquids* (Oxford University Press, New York, 1987).

<sup>28</sup>J. Chandrasekhar and W. L. Jorgensen, *J. Chem. Phys.* **77**, 5073 (1982).

<sup>29</sup>M. J. Bedard-Hearn, R. E. Larsen, and B. J. Schwartz, *J. Phys. Chem. A* **107**, 4667 (2003).

<sup>30</sup>M. J. Bedard-Hearn, R. E. Larsen, and B. J. Schwartz, *J. Phys. Chem. B* **107**, 14464 (2003).

<sup>31</sup>O. Steinhauser, *Mol. Phys.* **45**, 335 (1982).

<sup>32</sup>F. Webster, P. J. Rossky, and R. A. Friesner, *Comput. Phys. Commun.* **63**, 494 (1991).

<sup>33</sup>M. J. Bedard-Hearn, R. E. Larsen, and B. J. Schwartz, *J. Chem. Phys.* **123**, 234106 (2005).

<sup>34</sup>R. E. Larsen, M. J. Bedard-Hearn, and B. J. Schwartz, *J. Phys. Chem. B* **110**, 20055 (2006).

<sup>35</sup>M. J. Bedard-Hearn, R. E. Larsen, and B. J. Schwartz (unpublished).

<sup>36</sup>The reason we used three separate sections was based only on the fact that the data files containing these sections of the equilibrium run were the most easily accessible on the computer at the time when we were choosing the initial configurations.

<sup>37</sup>In MF-SD, the density matrix,  $\hat{\rho} = \sum_{j,k} a_j^* a_k |j\rangle\langle k|$ , undergoes stochastic decoherence events, which collapse the superposition state  $|\psi\rangle$  onto one of the adiabatic basis states, see Refs. 33 and 34.

<sup>38</sup>We say that the ground state is repopulated at time  $t_g$  when the density matrix element associated with the ground state,  $\rho_{00} = a_0^* a_0$ , has the majority of the population and remains so populated for all times afterward; that is,  $\rho_{00}(t) > 0.5 \forall t \in [t_g, \infty)$ .

<sup>39</sup>The charge densities shown in Figs. 1 and 3 are isodensity contours drawn at 10% of the maximum value using the free software CHIMERA, see Ref. 48.

<sup>40</sup>Even for trajectories in which the electron did not relocalize, diffusion caused  $\zeta(t)$  to decay to about 0.3 after several picoseconds.

<sup>41</sup>It is a coincidence that the electron happens to be localized in a disjoint cavity at  $t = 800$  fs [Figs. 3(A) and 3(E)] in the two trajectories shown in Figs. 2–4.

<sup>42</sup>K. A. Motakabbir and P. J. Rossky, *Chem. Phys.* **129**, 253 (1989).

<sup>43</sup>I. B. Martini and B. J. Schwartz, *Chem. Phys. Lett.* **360**, 22 (2002).

<sup>44</sup>D. Borgis, P. J. Rossky, and L. Turi, *J. Chem. Phys.* **125**, 064501 (2006).

<sup>45</sup>C. J. Smallwood, C. N. Mejia, W. J. Glover, R. E. Larsen, and B. J. Schwartz, *J. Chem. Phys.* **125**, 074102 (2006).

<sup>46</sup>T. H. Murphrey and P. J. Rossky, *J. Chem. Phys.* **99**, 515 (1993).

<sup>47</sup>E. A. Shaede, L. M. Dorfman, G. J. Flynn, and D. C. Walker, *Can. J. Chem.* **51**, 8434 (1973).

<sup>48</sup>C. C. Huang, G. S. Couch, E. F. Pettersen, and T. E. Ferrin, *Pac. Symp. Biocomput* **1**, 724 (1996); <http://www.cgl.ucsf.edu/chimera>